Jurnal Ilmiah PPI-UKM
Scientific Journal of PPI-UKM
Persatuan Pelajar Indonesia
Universiti Kebangsaan Malaysia
Selangor, Malaysia

Scientific Journal of PPI-UKM

Sciences and Engineering

ISSN No. 2356 - 2536

The Relationship Between PEM Fuel Cell Performance and Liquid Water Formation in The Anode and Cathode

Mulyazmi*
Department of Chemical Engineering, Bung Hatta University, Padang, Indonesia

Abstract

One factor that affects the performance of a PEM fuel cell is the water content in the fuel cell membrane. The membrane water content is influenced by the humidity of the reactants that flow into the cell. In this study, a membrane humidifier is used to control the relative humidity of reactants fed into a PEM fuel cell. The result was that liquid water on the anode side of PEM fuel cells occurred at temperatures from 353 to 363 K. At temperatures below 353 K, the water from the anode output was in the vapor phase. When the relative humidity at the cathode (RHC) and the relative humidity at the anode (RHA) were 90%, there was an increase in performance, and liquid water formation at the cathode occurred at temperatures from 303 K to 333 K. When the temperature was increased above 333 K, the effects on the cell performance and on the liquid water formation were not significant.

Keywords: Relative humidity; Liquid Water; Performance; PEM Fuel Cell

1. INTRODUCTION

Management of the water in the stack is an important problem in the operation and optimal performance of a fuel cell. It is necessary to balance the water in a fuel cell stack to ensure that the membrane remains in a hydrated state and to prevent flooding on the cathode side and dehydration of the anode side [3-5]. Several studies investigating the influence of water imbalances on PEM fuel cell systems have shown that small amounts of water in the stack will cause the membrane to become dry and cracked. Conversely, a significant amount of water will cause liquid, and consequently, the cathode side becomes flooded [6, 7]. The various roles of water in PEM fuel cell stacks are contradictory. Water is needed to ensure good conductivity for membrane protons. However, water also prevents protons from accessing the catalyst surface, which results in a lower reactivity value in the catalyst layer and thus increases the value of the activation polarization [8-10]. The water content in the membrane is determined by the balance between water production and water transport processes such as electro osmotic drag (EOD), which is related to the transfer of protons through the membrane, back diffusion from the cathode, and the diffusion of water between the oxidant and fuel [11, 12]. This study focuses on the liquid water formation flowing from the stack and the performance of PEM fuel cells. This condition is based on the balance of water in the system, which is affected by several factors, such as the relative humidity at the anode (RHA) and the cathode (RHC), the operating temperature and pressure, and the stoichiometric ratio of hydrogen and oxygen. The purpose of this study was to determine the effect of operating conditions on the performance of the system and the amount of liquid water flowing from the anode and cathode. The regulation of water balance settings can be predicted using a mathematical model.

2. DESIGN OF THE EXPERIMENT

In this study, a model was developed on the basis of several assumptions: the relative humidity of the gas exiting the membrane humidifier is similar to the relative humidity at the gas inlet of the fuel cell, all the reactant gases in the PEM fuel cell system are ideal gases, the PEM fuel cell system operates at a steady state, the PEM fuel cell system is under isothermal conditions, there are negligible pressure drops in the PEM fuel cell stack, The water flowing into the stack is in the gas phase.

To sufficiently hydrate the membrane, water is usually admitted into the cell by using various methods such as liquid injection, steam introduction, and humidifying reactants before they enter the cell. In this study, the method used involved adding an external humidifier to humidify the reactant gases before they flow into the cell, as shown in Fig. 1. The external humidifier used in this system is a type of membrane humidifier that does not require heat to generate steam to achieve the appropriate humidity. The membrane humidifier in this study performs two functions. The first function is to set the humidity of the hydrogen before it flows into the anode side at membrane humidifier 1(MH1).

* Corresponding author. Tel.: N/A; fax: N/A.
E-mail address: mulyazmi@yahoo.com.

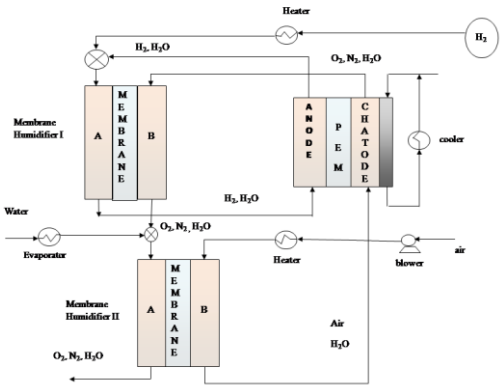

Fig. 1. Humidify the reactant gases before flow into the cell

The second function is to set the humidity of the oxygen before it flows into the cathode side at membrane humidifier 2 (MH2). The components that flow from the anode are hydrogen and water (vapor and liquid phase), and they are used again as reactants and fed to the anode side. Before entering the anode, hydrogen humidity control occurs in MH1. The water vapor used to control the humidity of the hydrogen is obtained from the water vapor from the cathode. The products flowing from the cathode are water (vapor and liquid phase), oxygen and nitrogen. The humidity of the air flowing from MH1 must be controlled at MH2 to achieve the appropriate humidity before it flows into the cathode side. The membrane water content depends on several factors, such as the relative humidity of the reactants on the anode side and the cathode side, the operating temperature and pressure, and the stoichiometric ratio of hydrogen and oxygen.

4. MATHEMATICAL MODEL

4.1 Water vapor in the reactants

Because the relative humidity φ, is the measured parameter in the experiment, it is necessary to know the relationship between the mole fraction and the relative humidity. The mole fraction of water vapor is defined as follows [30]:

$$y = \varphi \frac{P_{sat}}{P} \quad (1)$$

The amount of water vapor in the hydrogen supplied to the anode inlet is defined as follows:

$$\mathcal{N}_{H_2 O in H_2} = \frac{\delta_{H_2}}{2F} i . \eta_{cell} . \frac{\varphi . P_{V_s}}{P - \varphi . P_{V_s}} \quad (2)$$

The amount of water vapor in the oxygen supplied to the cathode inlet is defined as follows:

$$\mathcal{N}_{H_2 O in O_2} = \frac{\delta_{O_2}}{4F} i . \eta_{cell} \frac{\varphi . P_{V_s}}{P_a - \varphi . P_{V_s}} \quad (3)$$

The relative humidity at the anode and cathode are assumed to be 100% RH with no significant pressure drop. The concentrations of the water vapor at the anode and cathode gas outlets are defined as follows:

$$\mathcal{N}_{H_2 O in H_2, out} = \mathcal{N}_{H_2 unreac} . \eta_{cell} . \frac{P_{sat}}{P - P_{sat}} \quad (4)$$

$$\mathcal{N}_{H_2 O in air, out} = \mathcal{N}_{air, out} . \eta_{cell} \frac{P_{sat}}{P - P_{sat}} \quad (5)$$

4.2 Water diffusion in a PEM fuel cell

The number of protons that transfer from the anode to the cathode side by EOD $\mathcal{N}_{drag}$ can be calculated using the following equation [29, 31, 32]:

$$\mathcal{N}_{drag} = \frac{n_d}{F} i \quad (6)$$

where n_d is the coefficient of EOD; n_d can be defined using the following equation:

$$n_d = \frac{2.5\ \lambda pem}{22} \quad (7)$$

where λpem is thewater content ofthe membrane and can be calculated using the following equation:

$$\lambda = 0.0043 + 17.81 a_{H2O} - 39.85\, a_{H2O}^2 + 36 . a_{H2O}^3 \quad 0 < a_{H2O} \leq 1 \quad (8)$$

where a_{H2O} is the membrane water activity.

Hassan et al. [30] expressed the water that diffuses from the cathode side to the anode side as follows:

$$J_w = k_g (y_a - y_c) \quad (9)$$

where J_w is the moisture flux across the membrane, k_g is the mass transfer coefficient, y_a is the molar moisture content at the anode, and $y_c$is the molar moisture content on the cathode side.

4.3 Performance of a PEM fuel cell

The cell voltage value V_{oper} in the operation of a system is:

$$V_{oper} = V_{rev} - V_{irrev} \quad (10)$$

$$V_{irrev} = V_{act} - V_{ohm} - V_{con} \quad (11)$$

4.3.1 Reversible voltage (V_{rev})

The reversible voltage in a PEM fuel cell is [33-35]

$$V_{rev} = E_T + \frac{RT}{nF} ln\left(\frac{P_{H_2} x (P_{O_2}{}^{0.5})}{P_{H_2O}}\right) \quad (12)$$

The electrical potential at standard conditions is $E^0 = -\frac{\Delta G_f^0}{nF}$, and the electrical potential E_T in PEM fuel cells is:

$$E_T = 1.229V - 0.85 \times 10^{-3}(T - T_{ref})\frac{V}{K}$$

4.3.2 Activation voltage (V_{act})

The voltage loss by the activation is caused by the slow reaction taking place at the electrode surface. This loss occurs because the cell requires energy to transfer

electrons, namely, the activation energy that is required at the anode and the cathode[36]. The rate of reaction is:

$r = k_f C_{O_2} - k_b C_{H_2} = \frac{i_c}{nF} - \frac{i_a}{nF}$

If $i_c = i_a and r_f = r_b$, then equation (17) can be written as:

$$\frac{RT}{F}\left[\frac{d}{dE}\ln(k_b) - \frac{d}{dE}\ln\left(\frac{1}{k_f}\right)\right] = 1 \quad (13)$$

In the case of electron transfer, the two forms of equation (13) are aggregated into one factor, which is also known as a symmetry factor [22]. Using a symmetry factor (denoted as α) when oxygen is reduced, the following expression is obtained:

$$\ln\left(\frac{1}{k_f}\right) = \frac{\alpha FE}{RT} + c \quad (14)$$

For oxidative symmetry, the factor $1 - \alpha$ is used instead:

$\ln(k_b) = \frac{(1-\alpha)FE}{RT} + c$

Under standard conditions, $k_f = k_{f,0}$, $k_b = k_{b,0}$ and $E = E_0$. Equations (14) can be written as:

$$k_f = k_{f,0}\exp\left(\frac{-\alpha FE}{RT}\right) \quad (15)$$

and $k_b = k_{b,0}\exp\left(\frac{(1-\alpha)FE}{RT}\right)$ (16)

By substituting equations (15) and (16), which is also known as the Butler–Volmer equation, the reaction concentration in the cell becomes:

$$i = nF\left(k_{f,0}\exp\left(\frac{-\alpha FE}{RT}\right)C_{O_2} - k_{b,0}\exp\left(\frac{(1-\alpha)FE}{RT}\right)C_{H_2}\right) \quad (17)$$

At equilibrium, it is assumed that

$$k_{f,0} = k_{b,0}k_0 nF\left(k_0\exp\left(\frac{-\alpha FE_r}{RT}\right)C_{O_2}\right) = nF\left(k_0\exp\left(\frac{(1-\alpha)FE_r}{RT}\right)C_{H_2}\right) = i_0 \quad (18)$$

$$\left(\frac{C_{O_2}}{C_{H_2}}\right) = \exp\left(\frac{FE_r}{RT}\right) \quad (19)$$

By substituting equation (19) into equation (18), the The change in the current density is:

$$i_0 = nFk_0 C_{O_2}^{(1-\alpha)} C_{H_2}^{\alpha} \quad (20)$$

A comparison of Equation (21) with the reference current density $(i_{0,ref})$ yields:

$$\frac{i_0}{i_{0,ref}} = K_0\left(\frac{C_{O_2}}{C_{O_2,ref}}\right)^{(1-\alpha)}\left(\frac{C_{H_2}}{C_{H_2,ref}}\right)^{\alpha} \quad (21)$$

where

$k = Aexp\frac{E_c}{RT}$ and $\frac{k_0}{k_{0,ref}} = K_0$

The K_0 value at a given temperature relative to the reference temperature can be written as:

$$K_0 = exp\frac{E_c}{RT}\left(1 - \frac{T}{T_{ref}}\right) \quad (22)$$

Equation (22) can then be written as:

$$i_0 = i_{0,ref}\left(\frac{C_{O_2}}{C_{O_2,ref}}\right)^{(1-\alpha)}\left(\frac{C_{H_2}}{C_{H_2,ref}}\right)^{\alpha} exp\frac{E_c}{RT}\left(1 - \frac{T}{T_{ref}}\right) \quad (23)$$

The i_0 value influenced by the reaction surface as a per-unit volume of catalyst layer (a) is [37]

$$i_0 = ai_{0,ref}\left(\frac{P_R}{P_{R,ref}}^{\gamma}\right)exp\frac{E_c}{RT}\left(1 - \frac{T}{T_{ref}}\right) \quad (24)$$

R = reactant (H_2 and O_2) and

E_c = activation energy (76.5 kJ/mol) [38]. (41)

Song [39] defined the value of a as:

$$a = a_0\frac{m_{pt}}{L} \quad (25)$$

The value of a_0 was determine by Song [40] to be:

$a_0 = 10^8(4.4198Y^9 - 27.691Y^8 + 74.206Y^7 - 111.06Y^6 + 101.43Y^5 - 57.841Y^4 + 20.231Y^3 - 4.089Y^2 + 0.39451Y)$ (26)

where Y= % Pt.

According to Inoue [41]and Song [39], the reference current density is:

$$i_{0,ref} = 10^{\left(3.057 - \frac{4001}{T}\right)} \quad (27)$$

The current density from equation (17) is:

$$i = nFk_0\left(C_{O_2}\exp\left(\frac{-\alpha FE}{RT}\right) - C_{H_2}\exp\left(\frac{(1-\alpha)FE}{RT}\right)\right) \quad (28)$$

If i is compared with i_0, equation (20) becomes:

$$\frac{i}{i_0} = \frac{C_{O_2}}{C_{O_2}}\left(\exp\left(\frac{-\alpha FE}{RT}\right) + \left(\frac{\alpha FE_r}{RT}\right)\right) - \left(\exp\left(\frac{-\alpha FE}{RT}\right) + \left(\frac{\alpha FE_r}{RT}\right)\right)$$

For $E - E_r = \eta_{act}$, the $\frac{i}{i_0}$ value becomes:

$$V_{act} = \frac{RT}{2\alpha F}\sin h^{-1}\left(\frac{i}{i_0}\right) \quad (30)$$

The voltage activation [36, 42] is:

$$V_{act} = \frac{RT}{n\alpha F}\ln\left(\frac{i}{i_0}\right) where i > i_0 \quad (31)$$

According to Gorgun [42], the i_0 value is dependent on the temperature, pressure, type of catalyst, specific surface area and loading. The i_0 value ranges from 10^{-8}A to 10^{-2}A.The Tafel constant can be obtained:

$b = \frac{RT}{n\alpha F}$ where b = the Tafel constant.

The value of the Tafel constant is based on data obtained from a study conducted by Mann [43]and was determined based on the following expression:

$$b = 0.1937\ e^{-2.197(\alpha)} \quad (32)$$

The value of the exchange coefficient value α was obtained from Zhang [44]:

$$\alpha = (0.001552RH_{c,in} + 0.000139)T \quad (33)$$

$RH_{c,in}$ is the relative humidity of the reactants that flow into the cathode side. The over potential is caused by the reaction kinetics at the anode and the cathode because of the slow reduction of oxygen gas at the cathode. Therefore, the loss of voltage from the activation over potential is generally more dominant at the cathode [35].

4.3.3 Ohmic voltage (V_{ohm})

The loss caused by the ohmic resistance in the membrane and the catalyst layer is a function of temperature and humidity [37]. The ohmic voltage that is lost was presented by Kunusch [36] as:

$$V_{ohm} = iR_{ohm}$$ where the R_{ohm} value is:

$$R_{ohm} = \frac{t_m}{\sigma_m} \quad (34)$$

R_{ohm} is the resistance in the cell, which depends on the humidity and temperature of the cell membrane (V). The membrane proton conductivity can be written as [45, 46]

$$\sigma_m = (0.005139\,\lambda_m - 0.00326)\, exp\left[1268\left(\frac{1}{303} - \frac{1}{T}\right)\right] \quad (35)$$

where $\lambda_m$is the water content in the membrane.

$$\lambda_m = 0.048 + 17.81RH - 39.83aRH^2 + 39.85RH^3 \quad (36)$$

where RH is the average relative humidity in the cell.

4.3.4 Concentration voltage (V_{conc})

A concentration voltage loss occurs when the electrode reactions are hindered by the mass transfer of reactants into the cell [47] because the quantity of reactants required for the reaction is insufficient. The concentration voltage was presented by Shaker [34] as:

$$V_{conc} = \frac{RT}{nF} ln\left(\frac{i_L}{i_L - 1}\right) \quad (37)$$

where i_L= the limiting current density$\left(\frac{A}{cm^2}\right)$, which is the maximum current density. The limiting current density for the cell is [48]:

$$i_L = nF h_m \left(\frac{c_{O_{2,in}} - c_{O_{2,out}}}{ln\frac{c_{O_{2,in}}}{c_{O_{2,out}}}}\right) \quad (38)$$

$c_{O_{2,inandout}}$is the concentration of oxygen entering and exiting a cell (mol), and $h_m$is the convective mass transfer coefficient (m s^{-1}).

The convective mass transfer coefficient can be written as [49]: $$h_m = \frac{Sh_f D_{ij}}{H_c} \quad (39)$$

5. RESULTS AND DISCUSSION

The operating conditions used in the PEM fuel cell involve RHA and RHC values from 0 to 100%, changes in the current density from 0.1A/cm^2 to 0.9 A/cm^2, a stoichiometry ratio for hydrogen of 1.2 and for oxygen of 2, and a pressure at the anode and cathode of 1atm.

5.1 Effect of the relative humidity on the flow of condensed water from the anode

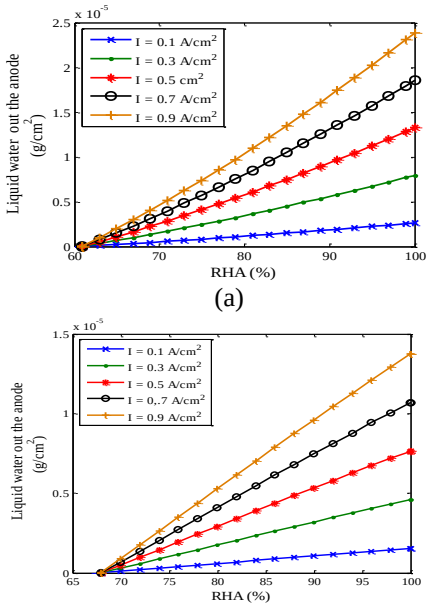

Fig. 2. The relationship between the RHA and liquid water from the anode at a temperature of 353 K:(a) RHC= 10% and (b) RHC= 30%

Fig. 2 shows the RHC is greater than 30%, then the water flowing from the anode side is in the vapor phase. Saturated water formed when the RHA was 60% and the RHC was 10% and when the RHA was 68% and the RHC was 30%. Fig. 3 shows the water flowing from the anode side at RHC values above 70% is in the vapor phase. Increases in the RHC affect the liquid water formation at values greater RHA. The operating conditions are as follows: the RHC is 10% and the RHA is 35**%**, the RHC is 50% and the RHA is 45%, and the RHC is 70% and the RHA is 55%. The water flowing from the anode side is in the vapor phase for all conditions under this RHA. Figs 2 and 3 show the flow of liquid water from the anode side of PEM fuel cells at temperatures from 353 to 363 K. At temperatures below 353 K, the water flowing from the anode side is in the vapor phase.

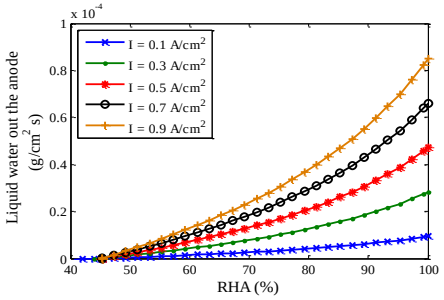

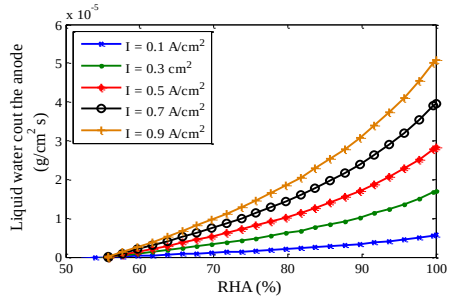

(b)

Fig. 3. The relationship between the RHA and liquid water from the anode at T 363 K: (a) RHC= 50% and(b) RHC=70%

5.2 Effect of the relative humidity on the flow of liquid water formation from the cathode

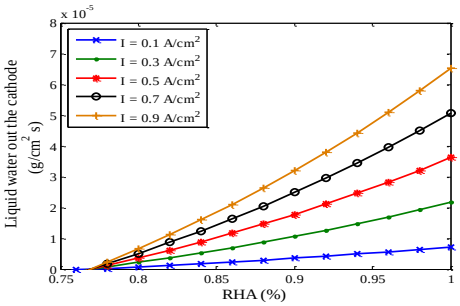

Fig. 4. The relationship between the RHA and liquid water from the cathode at a temperature of 363 K and 90% RHC

Fig. 4 shows the water flowing from the cathode is in the vapor phase if it has a maximum relative humidity of 100%. At a temperature of 363 K with a RHC of 90%, liquid water occurs when the RHA is in the range from 77% to 100%. Water saturation starts when the RHA is 77%. Below 77% RHA, the water flowing from the cathode is in the vapor phase. Fig. 5 shows the saturated water began to form on the cathode side of the PEM fuel cells at 75% RHC, and below this value, the water flowing from the cathode is in the vapor phase. At 90% RHC, all of the water flowing from the cathode is liquid water. This occurs because most of the water flowing from the cathode is at 90% RHC. The effect is that water forms directly, liquid water, and flows from the cathode side at low RHA.

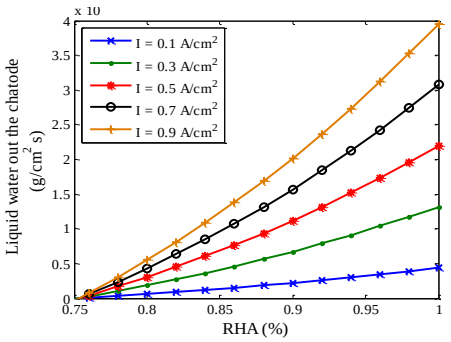

(a)

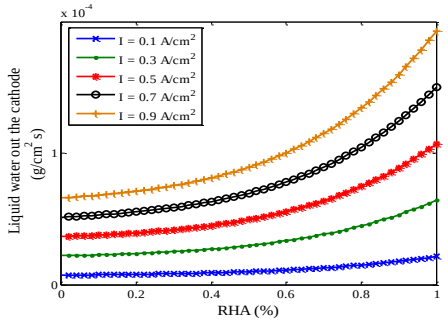

(b)

Fig. 5. The relationship between the RHA and liquid water from the cathode at a T 353 K: (a) RHC= 70% and (b) RHC= 90%

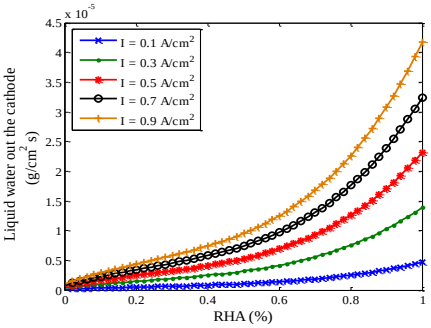

(a)

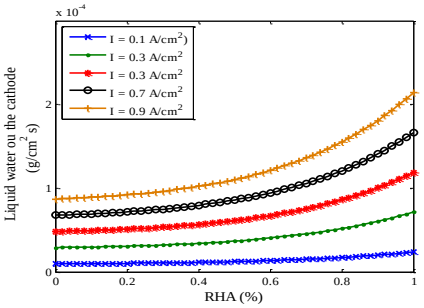

(b)

Fig. 6. The relationship between the RHA and liquid water from the cathode at T 343 K: (a) RHC= 50% and (b) RHC= 90%.

Fig. 6 shows at 50% RHC with 0% RHA, saturated water began to form. This describes the condition of the water flowing from the cathode that has a relative humidity of 100% and is saturated.

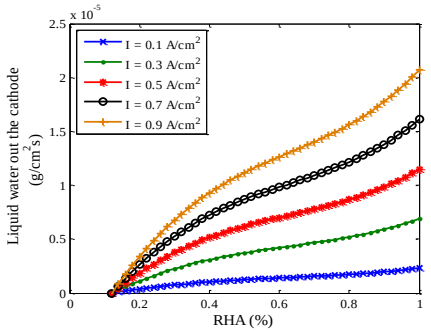

(a)

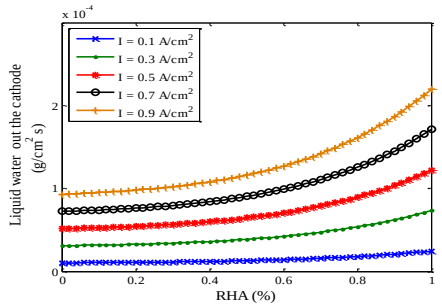

(b)

Fig. 7. The relationship between the RHA and liquid water liquid from the cathode at a temperature of 333 K: (a) RHC= 10% and (b) RHC= 90%

Fig. 7 shows the flow of liquid water from the cathode at a temperature of 333K. Increases in the RHC cause greater amounts of liquid water formation. Liquid water formed in the range from10 to 90% RHC for all values of the current density. When the RHC is 10%, liquid water occurs in the range from 12 to 100% RHA. Under 12% RHA, the water flowing from the anode side is in the vapor phase. At 90% RHC, liquid water occurs in the range from 0 to 100% RHA. Water flowing from the cathode side is liquid water if the RHC is 90%. The amount of liquid water varies and depends on the value of the current density. The amount of liquid water formation is higher when the value of the current density is large.

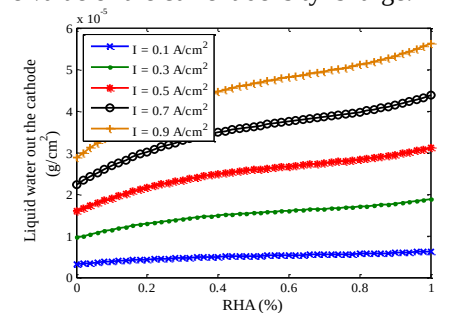

(a)

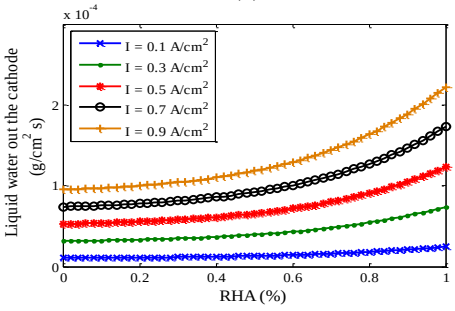

(b)

Fig. 8. The relationship between the RHA and liquid water from the cathode at a T 323 K: (a) RHC= 10% and (b) RHC= 90%

Fig. 8 shows the liquid water formation at a temperature of 323 K. Under these conditions, the liquid water occurs in the range from 10 to 90% RHC and from 0 to 100% RHA. The amount of liquid water formation at the lower RHA depends on the value of the current density. The higher the current density, the greater the amount of liquid water flowing from the cathodes of the PEM fuel cells. Figs 4 to 8 show that when the operating temperature decreases from 363 to 323 K, liquid water formation on the lower RHC. This condition occurs because at high temperatures, the amount of water vapor flowing out of the cell with the oxygen is unable to reach a relative humidity of 100%. A decrease in the operating temperature causes a lower amount of water vapor to be necessary to reach 100% relative humidity, and the liquid water increases.

5.3. Effects of voltage changes on liquid water at the anode when the current density is fixed

In this section, any change in the value of the voltage was followed by changes in the RHA, and the current density was fixed at 0.5A/cm^2.

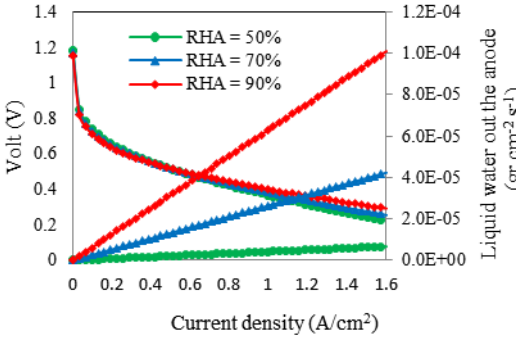

(a)

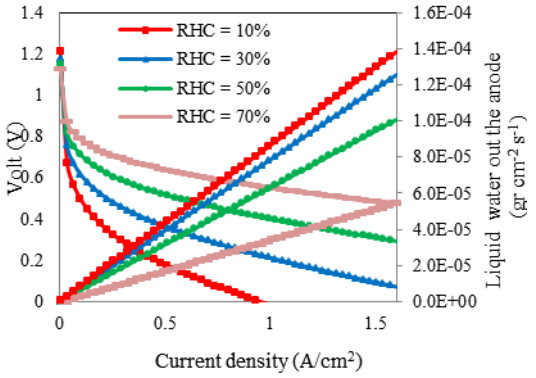

(b)

Fig. 9. The relationship between the performance and liquid water from the anode at a T 363 K: (a) 50%RHC, and (b) 90% RHA

Fig. 9 shows at a fixed RHC, a higher voltage results in the formation of a smaller amount of liquid water. After decreasing the voltage, the RHA was increased at the same current density. The result is an increase in the amount of water on the anode side when the voltage drops at a fixed current density. Increasing the RHC resulted in an increase in the value of the voltage produced. To achieve a high voltage, it is necessary for more water vapor from the anode side to move (together with protons) in the EOD phenomenon. As a result, the amount of water on the anode side is reduced, so the amount of liquid water flowing from the anode is reduced. A low amount of liquid water is obtained at 363 K with 58% RHA and 80% RHC, while the temperature of 353 K occurs at 17% RHA and 40% RHC.

At temperatures below 353 K, all of the water flowing from the anode side is in the vapor phase.

5.4. Effects of voltage changes on liquid water at the anode with changes in the current density

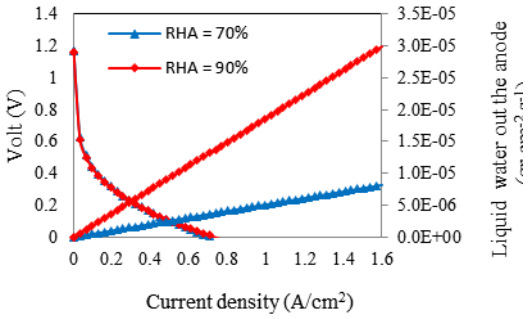

(a)

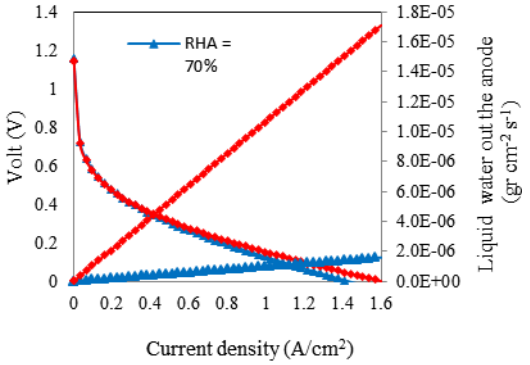

(b)

Fig. 10. The relationship between the performance and liquid water from the anode at T 353 K: (a) RHC= 10% and (b) RHC= 30%

Fig. 10 show the increasing the RHA did not cause a significant increase in the performance of the PEM fuel cells. Decreasing the value of the voltage or increasing the current density resulted in an increase in liquid water produced at the anode side of the fuel cell. Increase in the RHA resulted in an increase in the amount of liquid water flowing from the anode. This condition occurs due to an increase in the RHA and the water vapor flowing into the anode. The effect is an increase in liquid water formation. However, the increase in the RHC causes an increase in fuel cell performance and reduces the amount of liquid water on the anode side. This condition occurs because the increase in the RHC causes an increase in the average amount of water in the membrane such that more protons and more water vapor move from the anode side to the cathode side. The effect of increasing the RHC on cell performance is a change in the value of the maximum current density from 0.9 A/cm^2 at 10% RHC to 0.2 A/cm^2 at 50% RHC and 0.4 A/cm^2 at 90% RHC. Liquid water occurs only in the range from 50 to 90% RHA. Water flowing from the anode is in the vapor phase below 50% RHA. At 90% RHC, liquid water occurs only for 90% and 70% RHA. The water flowing from the anode is also in the vapor phase at 50% RHA.

Fig. 11 shows the RHC values above 30%, the water flowing from the anode is in the vapor phase. This condition indicates that above 30% RHC and below 70% RHA, water flows from the anode in the vapor phase. At a low RHC, PEM fuel cells have a current density of approximately 0.7 A/cm^2. However, when the RHC is increased to 30%, the current density approximately 1.4 A/cm^2, and at 70% RHC, it is approximately 1.6A/cm^2. that the liquid water from the anode side is formed at 353 and 363 K. At both of these temperatures under 70% RHA, the water flowing from the anode is in the vapor phase.

5.5. Influence of the performance of PEM fuel cells on liquid water formation at the cathode

Fig. 12 shows the increased temperatures also affect the decrease in the amount of liquid water flowing from the cathode. This condition occurs because increasing temperatures cause increases in the amount of water in the vapor phase to achieve 100% relative humidity. As a result of this condition, the amount of water in the liquid phase flowing out the cathode is lower at higher operating temperatures. The increase in the RHA causes an increase in the amount of liquid water flowing from the cathode. This condition occurs due to an increased RHA, resulting in a small increase in the performance of PEM fuel cells. This condition can occur when the RHA is increased from 10 to 90% at 323 K, which causes the maximum current density to increase from 0.13 A/cm^2 to 0.19 A/cm^2. Increases in the performance of the PEM fuel cell are shown by the increase in the amount of water vapor moving with protons in the EOD phenomenon. The effect of the increased performance is the production of more water in the reaction. Increasing the RHA caused an increase in liquid water formation. This behavior is observed at 50 and 90% RHA. Under these conditions, liquid water occurs from 303 to 333 K. At temperatures above 333 K, all the water flowing from the cathode is in the vapor phase. The current density at each condition shows that the resulting liquid water tends to have the same value even if there are differences in the RHC. The current density at each operating temperature is relatively similar, although the RHA values differ. The amount of liquid water formation at 90% RHC and 333 K is less than that at temperatures below 333 K. The amount of liquid water flowing from the cathode is higher when the current density is large.

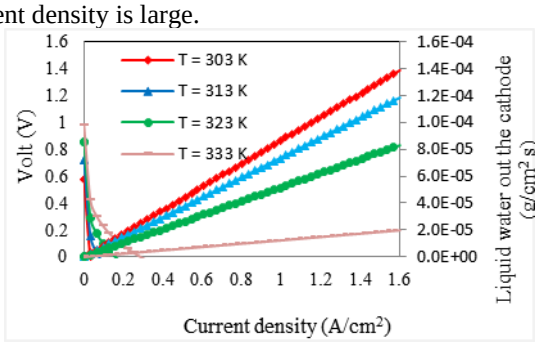

(a)

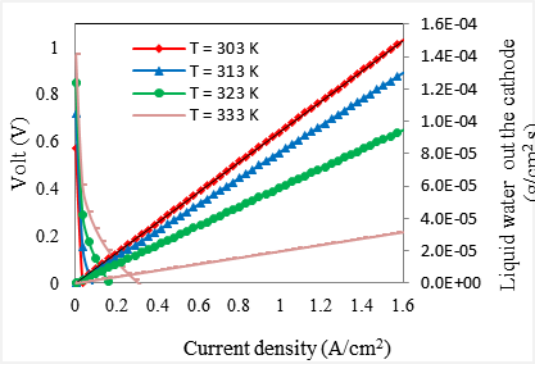

(b)

Fig. 11. The relationship between the performance and liquid water from the cathode at 10% RHC:RHA = 50%, and (b) RHA = 90%

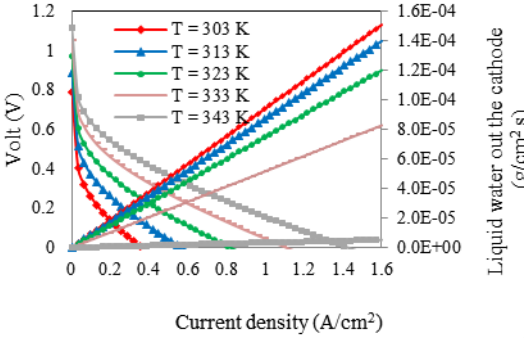

(a)

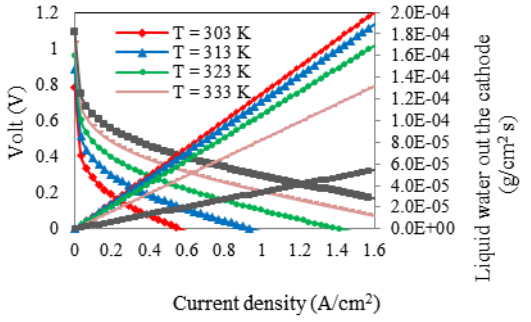

(b)

Fig. 12. The relationship between the performance and liquid water from the cathode at 50% RHC:(a) RHA =10%, (b) RHA= 90%

In Fig. 12, increases in the RHA causes liquid water to increase significantly. This behavior results in an increase in the amount of water flowing from the cathode side. The source of the water is the reaction. Increasing the operating temperature results in a decrease in the amount of liquid water flowing from the cathode. At temperatures from 303 to 333 K, increased operating temperatures increase the fuel cell performance. The operating temperature increases with the current density below 0.6 A/cm^2 showed a slightly increase in the amount of liquid water. Mean while, the temperatures of 333 and 343 K showed an increase in the amount of liquid water formation. This is evidenced by the high voltage and current density values.

Fig. 13 shows the performance of PEM fuel cells increased, especially from 303 to 333 K. However, for temperatures above 333 K, the increases in performance were not significant. At 10% RHA and 343 and 353 K, the performance of the PEM fuel cells is slightly different. The cell performance is almost the same at 50% RHA. The fuel cell performance is the same at 90% RHA for operating temperatures of 353 K and 363 K, and the tendency is the same at 343 K. This condition indicates that the increases in the RHA, the RHC and the temperature have no effect on the increase in the performance of the PEM fuel cells. When the RHA is 10, 70 and 90% and the temperature is 303, 313 and 323 K, the amount of liquid water flowing from the cathode is the same. At 343 and 353 K with 90% RHA, the same amount of water has a current density below 1 A/cm^2. However, above 1A/cm^2, there is little difference in the amount of liquid water formation.

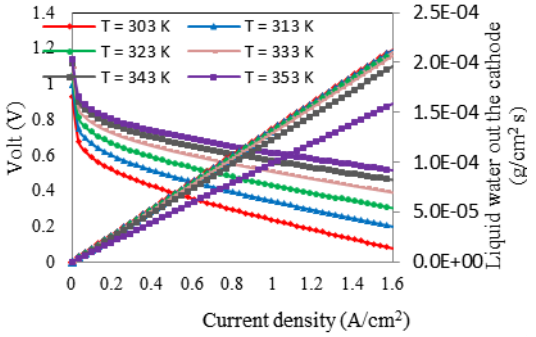

(a)

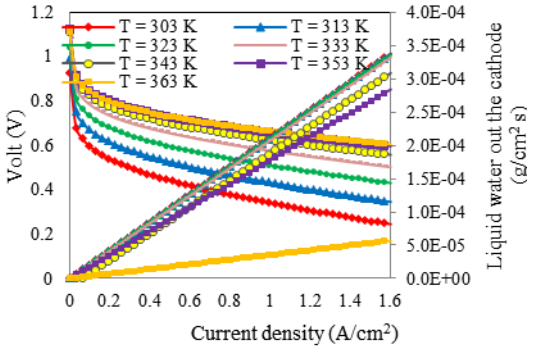

(b)

Fig. 13. The relationship between the performance and liquid water from the cathode at 90% RHC:(a)RHA = 50%, and (b) RHA= 90%

5.6 Comparison of the amount of liquid water

The results of this investigation were compared with experiments performed Cai [50]. The operating conditions in the system are shown in Table1. The increase in the relative water content in the anode causes an increased concentration of liquid water in the cathode. Fig. 14 shows the relationship between the current density and the total amount of water produced at the cathode. The conditions for the system operations are shown in Table 1. The increase in current density resulted in a higher total amount of water in the cathode, and increasing the RHA from 0 to 75% caused an increase in the total amount of water in the cathode.

Table 1
Research data used by Cai [50]

Parameter	Value (by Cai)
Relative humidity at cathode (RHC)	56%
Relative humidity at anode (RHA)	0% and 75%
Pressure at anode (PA)	2 atm
Pressure at cathode (PC)	2 atm
Cuurent density (i)	
Temperature (T)	333 K
Stoichiometry of hydrogen	1.1
Stoichiometry of oxygen	2.5
The active area of MEA	128 cm^2
Membrane Type	Nafion 112
Active area of MEA	128 cm^{-2}
Membrane thickness	0.0005 cm
Current density	0.5 A cm^{-2}

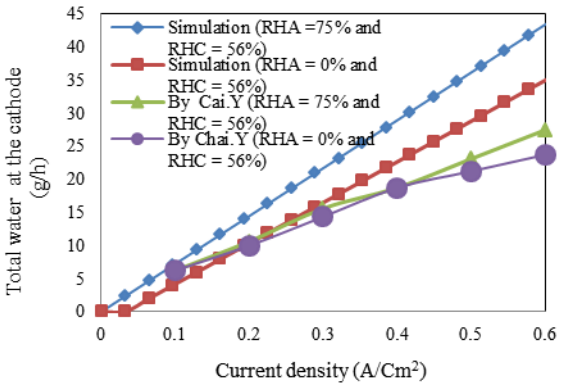

Fig. 14. Comparison between this investigation with the study by Cai (2006)

6. CONCLUSIONS

1. Increasing the RHA causes an increase in the liquid water formation flowing from the anode and cathode, and increasing the RHC decreases the liquid water in the anode and increases liquid water in the cathode.

2. Liquid water on the anode side of the cell occurs in the temperature range from 353 to 363 K. At temperatures below 353 K, the water flowing from the anode is in the vapor phase. Liquid water formation at a temperature of 353 K occurs in the range from 10 to 30% RHC and from 61 to 100% RHA. At 363 K, liquid water occurs between10 and 70% RHC and from 35 to 55% RHA.
3. Decreasing the operating temperature from 363 to 323K on the cathode side causes liquid water to occur at lower RHC values.

4. At 90% RHC and RHA, an increase in performance and liquid water from the cathode occurs at temperatures from 303 to 333 K. Increasing the temperature above 333 K did not have a significant effect on the performance and liquid water formation, and their values did not change.

NOMENCLATURE

a	Surface area to unit volume ratio of the catalyst layer $\left(\frac{cm^2}{cm^3}\right)$
a_0	Total surface area of the catalyst per unit mass of catalyst $\left(\frac{cm}{g}\right)$
b	Tafel constant
C	Concentration (mol)
D_{ij}	Binary diffusion coefficient of O_2 in N_2 (cm/s)
E	Electrical potential (V)
E^o	Electrical potential at standard conditions (V)
E_T	Electrical potential of PEM fuel cells (V)
F	Faraday constant (96,485 C/mol electrons)
G	Gibbs free energy (J/mol)
H	Enthalpy (J)
H_c	Hydraulic diameter (cm)
h_m	Convective mass transfer coefficient (m s^{-1})
i	Current density (A cm^{-2})
i_o	Exchange current density (A cm^{-2})
i_L	Limiting current density(A cm^{-2})
$i_{o,ref}$	References current density (A cm^{-2})
k	Reaction rate constant
L	Thickness of catalyst(cm)
m_{pt}	Catalyst load $\left(\frac{g}{cm^2}\right)$
n	Number of electrons per hydrogen molecule
n_{cell}	Number of cells
N	Concentration (mol)
P	Pressure (atm)
P_i	Partial pressure (atm)
Q	Charge (Coulombs / mol)
R	Universal gas constant (J/mol K)
r	Reaction rate (mol/cm^2 s)
RH	Average relative humidity
$RH_{c,in}$	Relative humidity of the reactants flowing into the cathode
R_{ohm}	Resistance in the cell (Ω)
S	Entropy (J/g K)
Sh_f	Sherwood number
T	Temperature (K)
t_m	Dry membrane thickness (cm)
T_{ref}	Reference temperature (K)
V	Voltage (V)
W_{el}	Maximum electrical work(J/mol)
X_{H2O}	Vapor mole fraction of H_2O
X_{O_2}	Mole fraction of oxygen
Y	Pt percentage (%)

Greek letters

α	Exchange coefficient
λ	Membrane water content
σ_m	Membrane proton conductivity (S cm^{-1})
Δ	Delta
ε	Stoichiometry

References

[1] Baschuk JJ, Li X. A general formulation for a mathematical PEM fuel cell model. Journal of Power Sources. 2005;142:134-53.
[2] Wu J, Zi Yuan X, Wang H, Blanco M, Martin JJ, Zhang J. Diagnostic tools in PEM fuel cell research: Part II: Physical/chemical methods. International Journal of Hydrogen Energy. 2008;33:1747-57.
[3] Baschuk JJ, Li X. Modelling of polymer electrolyte membrane fuel cells with variable degrees of water flooding. Journal of Power Sources. 2000;86:181-96.
[4] BiyIkoglu A. Review of proton exchange membrane fuel cell models. International Journal of Hydrogen Energy. 2005;30:1181-212.
[5] Chang H, Kim JR, Cho JH, Kim HK, Choi KH. Materials and processes for small fuel cells. Solid State Ionics. 2002;148:601-6.
[6] Falcão DS, Oliveira VB, Rangel CM, Pinho C, Pinto AMFR. Water transport through a PEM fuel cell: A one-dimensional model with heat transfer effects. Chemical Engineering Science. 2009;64:2216-25.

[7] Guvelioglu GH, Stenger HG. Flow rate and humidification effects on a PEM fuel cell performance and operation. Journal of Power Sources. 2007;163:882-91.
[8] Stumper J, Löhr M, Hamada S. Diagnostic tools for liquid water in PEM fuel cells. Journal of Power Sources. 2005;143:150-7.
[9] Liu X, Guo H, Ma C. Water flooding and two-phase flow in cathode channels of proton exchange membrane fuel cells. Journal of Power Sources. 2006;156:267-80.
[10] Liu Z, Mao Z, Wang C. A two dimensional partial flooding model for PEMFC. Journal of Power Sources. 2006;158:1229-39.
[11] Kraytsberg A, Ein-Eli Y. PEM FC with improved water management. Journal of Power Sources. 2006;160:194-201.
[12] Yan W-M, Chen C-Y, Mei S-C, Soong C-Y, Chen F. Effects of operating conditions on cell performance of PEM fuel cells with conventional or interdigitated flow field. Journal of Power Sources. 2006;162:1157-64.
[13] Janssen GJM, Overvelde MLJ. Water transport in the proton-exchange-membrane fuel cell: measurements of the effective drag coefficient. Journal of Power Sources. 2001;101:117-25.
[14] Lee Y, Kim B, Kim Y. An experimental study on water transport through the membrane of a PEFC operating in the dead-end mode. International Journal of Hydrogen Energy. 2009;34:7768-79.
[15] Liu F, Lu G, Wang C-Y. Water transport coefficient distribution through the membrane in a polymer electrolyte fuel cell. Journal of Membrane Science. 2007;287:126-31.
[16] Park YH, Caton JA. An experimental investigation of electro-osmotic drag coefficients in a polymer electrolyte membrane fuel cell. International Journal of Hydrogen Energy. 2008;33:7513-20.
[17] Yousfi-Steiner N, Moçotéguy P, Candusso D, Hissel D, Hernandez A, Aslanides A. A review on PEM voltage degradation associated with water management: Impacts, influent factors and characterization. Journal of Power Sources. 2008;183:260-74.
[18] Sun H, Zhang G, Guo L-J, Dehua S, Liu H. Effects of humidification temperatures on local current characteristics in a PEM fuel cell. Journal of Power Sources. 2007;168:400-7.
[19] Saleh MM, Okajima T, Hayase M, Kitamura F, Ohsaka T. Exploring the effects of symmetrical and asymmetrical relative humidity on the performance of H2/air PEM fuel cell at different temperatures. Journal of Power Sources. 2007;164:503-9.
[20] Okada T. Theory for water management in membranes for polymer electrolyte fuel cells: Part 1. The effect of impurity ions at the anode side on the membrane performances. Journal of Electroanalytical Chemistry. 1999;465:1-17.
[21] Spernjak D, Prasad AK, Advani SG. Experimental investigation of liquid water formation and transport in a transparent single-serpentine PEM fuel cell. Journal of Power Sources. 2007;170:334-44.
[22] Barbir F, Gorgun H, Wang X. Relationship between pressure drop and cell resistance as a diagnostic tool for PEM fuel cells. Journal of Power Sources. 2005;141:96-101.
[23] Rao RM, Bhattacharyya D, Rengaswamy R, Choudhury SR. A two-dimensional steady state model including the effect of liquid water for a PEM fuel cell cathode. Journal of Power Sources. 2007;173:375-93.
[24] Ma HP, Zhang HM, Hu J, Cai YH, Yi BL. Diagnostic tool to detect liquid water removal in the cathode channels of proton exchange membrane fuel cells. Journal of Power Sources. 2006;162:469-73.
[25] Li H, Tang Y, Wang Z, Shi Z, Wu S, Song D, et al. A review of water flooding issues in the proton exchange membrane fuel cell. Journal of Power Sources. 2008;178:103-17.
[26] Amirinejad M, Rowshanzamir S, Eikani MH. Effects of operating parameters on performance of a proton exchange membrane fuel cell. Journal of Power Sources. 2006;161:872-5.
[27] Park S-K, Choe S-Y, Choi S-h. Dynamic modeling and analysis of a shell-and-tube type gas-to-gas membrane humidifier for PEM fuel cell applications. International Journal of Hydrogen Energy. 2008;33:2273-82.
[28] Li X, Sabir I. Review of bipolar plates in PEM fuel cells: Flow-field designs. International Journal of Hydrogen Energy. 2005;30:359-71.
[29] Zhou B, Huang W, Zong Y, Sobiesiak A. Water and pressure effects on a single PEM fuel cell. Journal of Power Sources. 2006;155:190-202.
[30] Hassan NSM, Daud WRW, Sopian K, Sahari J. Water management in a single cell proton exchange membrane fuel cells with a serpentine flow field. Journal of Power Sources. 2009;193:249-57.
[31] Zong Y, Zhou B, Sobiesiak A. Water and thermal management in a single PEM fuel cell with non-uniform stack temperature. Journal of Power Sources. 2006;161:143-59.
[32] Yu X, Zhou B, Sobiesiak A. Water and thermal management for Ballard PEM fuel cell stack. Journal of Power Sources. 2005;147:184-95.
[33] Placca L, Kouta R, Blachot J-F, Charon W. Effects of temperature uncertainty on the performance of a degrading PEM fuel cell model. Journal of Power Sources. 2009;194:313-27.
[34] Shaker H. Analytical modeling of PEM fuel cell i–V curve. Renewable Energy. 2011;36:451-8.
[35] Chen Y-S, Peng H. A segmented model for studying water transport in a PEMFC. Journal of Power Sources. 2008;185:1179-92.
[36] Kunusch C, Puleston PF, Mayosky MA, Moré JJ. Characterization and experimental results in PEM fuel cell electrical behaviour. International Journal of Hydrogen Energy. 2010;35:5876-81.
[37] Scott K, Mamlouk M. A cell voltage equation for an intermediate temperature proton exchange membrane fuel cell. International Journal of Hydrogen Energy. 2009;34:9195-202.
[38] Wei Suna BAP, Kunal Karana. An improved two-dimensional agglomerate cathode model to study the nfluence of catalyst layer structural parameters
Electrochemica Acta. 2005;50:16.
[39] Song D, Wang Q, Liu Z, Navessin T, Eikerling M, Holdcroft S. Numerical optimization study of the catalyst layer of PEM fuel cell cathode. Journal of Power Sources. 2004;126:104-11.
[40] Song D, Wang Q, Liu Z, Eikerling M, Xie Z, Navessin T, et al. A method for optimizing distributions of Nafion and Pt in cathode catalyst layers of PEM fuel cells. Electrochimica Acta. 2005;50:3347-58.
[41] Inoue G, Matsukuma Y, Minemoto M. Evaluation of the optimal separator shape with reaction and flow analysis of polymer electrolyte fuel cell. Journal of Power Sources. 2006;154:18-34.
[42] Görgün H, Arcak M, Barbir F. An algorithm for estimation of membrane water content in PEM fuel cells. Journal of Power Sources. 2006;157:389-94.
[43] Mann RF, Amphlett JC, Peppley BA, Thurgood CP. Application of Butler–Volmer equations in the modelling of activation polarization for PEM fuel cells. Journal of Power Sources. 2006;161:775-81.
[44] Zhang J, Tang Y, Song C, Xia Z, Li H, Wang H, et al. PEM fuel cell relative humidity (RH) and its effect on performance at high temperatures. Electrochimica Acta. 2008;53:5315-21.
[45] Zhang X, Guo J, Chen J. The parametric optimum analysis of a proton exchange membrane (PEM) fuel cell and its load matching. Energy. 2010;35:5294-9.
[46] Shan Y, Choe S-Y. A high dynamic PEM fuel cell model with temperature effects. Journal of Power Sources. 2005;145:30-9.
[47] Abdellah B. Modeling and simulation of proton exchange membrane fuel cell systems. Journal of Power Sources. 2012;205:335-9.
[48] C. Spiegel. PEM Fuel Cell Modeling and Simulation Using MATLAB. Elsevier Inc. 2008.
[49] B. Tavakoli RR. The effect of fuel cell operational conditions on the water content distribution in
the polymer electrolyte membrane. Renewable Energy. 2011;XXX:13.
[50] Cai Y, Hu J, Ma H, Yi B, Zhang H. Effect of water transport properties on a PEM fuel cell operating with dry hydrogen. Electrochimica Acta. 2006;51:6361-6.